

## CHAPTER 6

### Storms and weather windows

The synoptic variability of wind waves is traced back to the frequency of passage of atmospheric disturbances, their strength, the duration of their action on the water surface and the geographic properties of the area. The variability manifests itself as a sequence of alternating storms and weather windows, which can be represented formally (see Fig. 1.1) as a sequence of positive (a storm) and negative (a weather window) fluctuations of the random process  $\xi(t)$  relative to some fixed value  $Z$ .

Let  $h(t)$  denote wave heights measured at synoptic observation times.  $\mathfrak{I}$  and  $\Theta$  denote the duration of a period when wave height deviations from  $Z$  were positive and negative, respectively.

Then the maximum wave height during the storm is

$$h^+ = \max_{0 \leq t \leq \mathfrak{I}} \{\xi(t)\} \quad (6.1)$$

The minimal wave height during the weather window is

$$h^- = \min_{0 < t < \Theta} \{\xi(t)\} \quad (6.2)$$

A system of the four interconnected random variables  $\Xi = (h^+, h^-, \mathfrak{I}, \Theta)$  can be used to parameterize the pulse-like stochastic process shown in fig. 1.1.

Table 6.1 gives a description of the data series that were used to study the synoptic variability of wind wave heights [Rozhkov et al., 1999; Boukhanovsky, Lavrenov et al., 1999].

**Table 6.1.**  
*Data used in computation of storms and weather windows*

Sea	$\varphi, \lambda$	Depth, (m)	Record Length, years	Parameters of distribution (1.5)					
				Annual means		Winter	Spring	Summer	Autumn
				$h_{0.5},$ (cm)	s	$h_{0.5}$ (cm), s	$h_{0.5}$ (cm), s	$h_{0.5}$ (cm), s	$h_{0.5}$ (cm), s
Baltic	55°20' 20°30'	30	1957-1991	66	1.8	77 1.7	60 2.0	55 2.3	75 1.8
Black	43°10' 34°00'	2200	1954-1988	73	2.5	92 2.1	73 2.9	60 3.8	72 2.8
Mediterranean	35°10' 35°05'	1070	1980-1994	60	2.6	75 2.2	65 2.8	51 4.3	54 3.2
Barents	71°05' 35°09'	180	1980-1989	119	2.0	143 2.2	115 2.1	97 2.2	129 2.1

For  $h(t)$  a multi-year long (10-35 years) time series of mean wave height was taken as simulated by a wave model. The model was driven at regular synoptic times by gridded atmospheric pressure fields. The computations represented a variety of physiographic conditions in internal and marginal seas.

Table 6.2 provides mean ( $m$ ) and root mean square deviation ( $\sigma$ ) values of four-variable random functions  $\Xi$  that were computed using samples from a sequence of storms (from 150 to 1000 storms).

The threshold value  $Z$  was taken, correspondingly, equals to quantiles  $h_{0.5}, h_{0.25}, h_{0.75}, h_{0.9}$ . The breakdown of values is done by seasons, so that synoptic variations of the wind wave fields are described taking into account the annual cycle.

It can be seen from the table 6.2 that for  $Z=h_{0.5}$  the average storm duration  $\mathfrak{I}$  is two days, while the average duration of weather window  $\Theta$  is 2–3 days. For larger values of  $Z$ , such as  $h_{0.75}$ ,  $\mathfrak{I}$  is reduced to one day, and  $\Theta$  increases.

Random functions  $\mathfrak{I}$  and  $\Theta$  represent duration of over-shots and under-shots. Therefore their distributions should asymptotically tend to the exponential law [Leadbetter, 1986]:

$$F(x) = 1 - \exp\left(-\frac{x}{\bar{x}}\right) \quad (6.3)$$

Figs. 6.1 and 6.2 depict quantiles of distributions  $F^*(\mathfrak{I})$  and  $F^*(\Theta)$  as the  $q$ - $q$  bi-plots. It can be seen that the hypothesis that  $F^*(x)$  belongs to a class of exponential distributions is confirmed. Hence  $m$  and  $\sigma$  should be nearly equal (as seen from Table 6.2). Table. 6.3 gives correlation coefficients between different random functions in system  $\Xi$ .

**Table 6.2**

Estimates of means ( $m$ ) and r.m.s. ( $\sigma$ ) of the highest mean waves  $h_+$  in storms, lowest mean waves  $h_-$  in weather windows, duration of storms  $\mathfrak{S}$  and duration of weather windows  $\Theta$  for thresholds  $Z$  that correspond to different quantiles of wave height climatic distributions (left column)

%	Z, (cm)	$h_+$ , (cm)		$h_-$ , (cm)		$\mathfrak{S}$ , (hours)		$\Theta$ , (hours)		N
		$m$	$\sigma$	$m$	$\sigma$	$m$	$\sigma$	$m$	$\sigma$	
<b>WINTER (XII,I,II)</b>										
<b>Baltic sea</b>										
25%	53	124	75	37	12	72	79	31	32	653
50%	77	145	73	43	17	55	56	59	60	615
75%	114	185	66	54	30	39	37	111	125	434
<b>Black sea</b>										
50%	92	175	76	61	17	46	38	58	57	656
75%	126	200	72	67	25	34	28	92	95	517
<b>SPRING (III,IV,V)</b>										
<b>Baltic sea</b>										
25%	43	92	52	32	9	70	76	28	26	793
50%	60	105	49	40	15	40	41	57	60	792
75%	83	131	51	40	21	34	33	130	148	482
<b>Black sea</b>										
50%	73	110	49	55	11	37	40	61	62	794
75%	91	141	54	56	18	33	34	159	188	409
<b>SUMMER (VI,VII,VIII)</b>										
<b>Baltic sea</b>										
25%	42	80	34	32	10	61	59	30	30	852
50%	55	84	32	36	12	43	42	42	43	915
75%	74	104	32	38	18	31	27	115	126	518
<b>Black sea</b>										
50%	60	80	17	49	11	39	39	61	71	806
75%	72	88	17	52	15	28	26	120	158	558
<b>AUTUMN (IX,X,XI)</b>										
<b>Baltic sea</b>										
25%	51	117	71	37	11	75	88	33	30	704
50%	75	139	68	44	17	56	61	64	70	623
75%	109	173	63	54	27	43	39	106	131	480
<b>Black sea</b>										
50%	72	110	45	55	13	38	36	59	62	751
75%	91	141	47	56	18	34	28	132	146	393

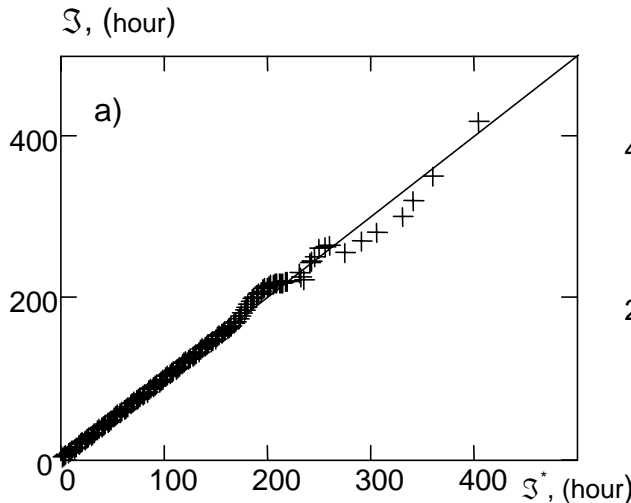


**Figure 6.1.** Empirical distribution of storm duration  $F(\mathfrak{S})$  /quantile bi-plot of exponential distribution (6.3)/. The Baltic Sea.

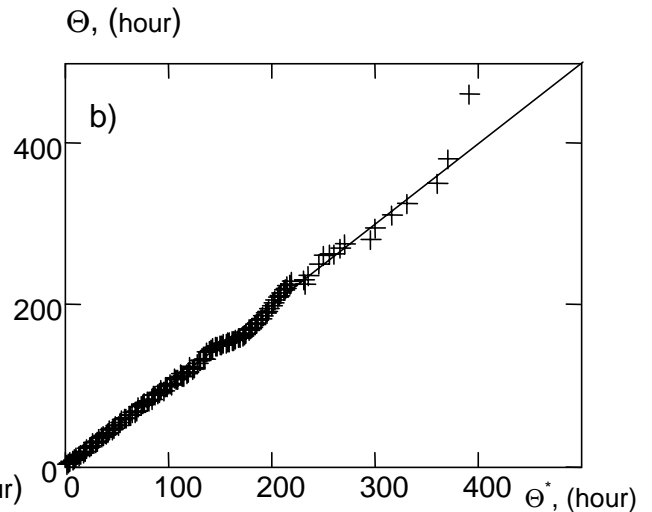


**Figure 6.2.** Empirical distribution of weather window duration  $F(\Theta)$  /quantile bi-plot of exponential distribution (6.3)/. The Baltic Sea.

**Table 6.3**  
Correlation coefficients  $\rho$  between impulse parameters

Values	(h+,h-)	(h+,Θ)	(h-,Ξ)	(Ξ,Θ)	(h+,Ξ)	(h-,Θ)
$\rho$	-0.1±0.15	-0.15±0.05	-0.1±0.1	-0.1±0.1	0.5±0.8	-0.55±-0.7

Hence, in the first approximation it is possible to consider parameters  $(h+, h-), (h+, \Theta), (h-, \Xi), (\Xi, \Theta)$  independent while parameters  $(h-, \Theta), (h+, \Xi)$  are dependent because their correlation coefficient is in the range of 0.5–0.8.

Hence, the four-dimensional distribution  $F(h+, h-, \Xi, \Theta)$  can be expressed as a product of two two-dimensional distributions  $F(h+, \Xi)$  and  $F(h-, \Theta)$ , each of them being equal to

$$F(x, y) = F(x)F(y|x) \quad (6.4)$$

i.e. to multiplication of the marginal distribution  $F(x)$  and conditional distribution  $F(y|x)$  where  $x = \{\Xi, \Theta\}$  and  $y = \{h+, h-\}$ .

It follows from definitions (6.1) and (6.2), that the values  $h+$  and  $h-$  are extreme values in a sample, so the asymptotic distributions of  $F(h+)$  and  $F(h-)$  are close to relations (2.2) - (2.4).

For example, the distribution of  $h+$  should asymptotically tend towards

$$F(h^+ | \Xi) = \begin{cases} \exp\left[-\exp\left(-\frac{h^+ - A(\Xi)}{B(\Xi)}\right)\right], & h^+ \geq Z \\ 0, & h^+ < Z \end{cases} \quad (6.5)$$

where  $A(\Xi)$  and  $B(\Xi)$  are parameters depending on the conditional moments  $m(\Xi), \sigma(\Xi)$  via the following relations

$$\begin{aligned} B(\Xi) &= \frac{\sqrt{6}}{\pi} \sigma(\Xi), \\ A(\Xi) &= m(\Xi) - 0.5772B(\Xi) \end{aligned} \quad (6.6)$$

Empirical conditional distributions  $F(h^+|\Xi)$  are compared with approximation (6.5) in Fig. 6.3. It can be seen that approximation (6.5) is acceptable. Parameters  $A$  and  $B$  for various seas are presented in Table 6.4.

In [Angelides et al., 1981; Boukhanovsky, Lopatoukhin, Ryabinin, 1998] distributions of  $h^+$  are approximated using a family of 3-parameter Weibull distributions

$$F(y/x) = 1 - \exp\left[-\left(\frac{y - Z}{A(x) - Z}\right)^{B(x)}\right] \quad (6.7)$$

where the third parameter  $Z$  determines the threshold, and two first parameters  $A$  and  $B$  are estimated using data in the sample. In those papers a constant value  $Z=1.0$  m was adopted for all seasons. Distribution (6.5) with parameters  $A$  and  $B$  from Table 6.4, which are dependant on season, function  $\Xi$ , and on variable  $Z$ , is more accurate than the previous approximation (6.7).

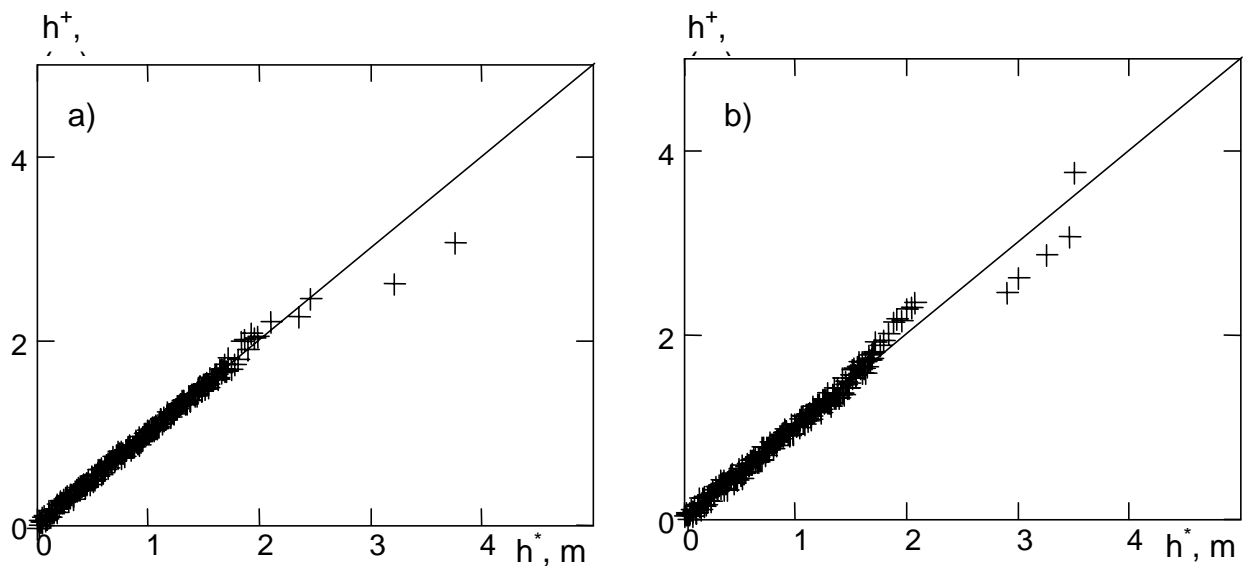


**Figure 6.3.** Empirical conditional distribution  $h^+$  (m) of highest waves in storms of different duration  $\Xi$ /quantile bi-plot of distribution (6.5)/, a:  $\Xi \leq 50$  hours, b:  $50 < \Xi \leq 100$  hours. Baltic Sea.

**Table 6.4.**  
Parameters A and B of distribution (6.5) for cold and warm seasons and various seas

$\mathcal{S}$ , (hours)	Winter		Summer		Winter		Summer		
	A, (m)	B, (m)	A, (m)	B, (m)	A, (m)	B, (m)	A, (m)	B, (m)	
<b>The Black Sea</b>				<b>The Mediterranean Sea</b>					
0-25	0.19	0.24	0.06	0.05	0.12	0.17	0.04	0.05	
25-50	0.51	0.61	0.11	0.12	0.43	0.48	0.09	0.12	
50-75	0.60	0.53	0.10	0.12	0.56	0.66	0.13	0.12	
>75	0.71	0.60	0.08	0.19	0.50	0.37	0.09	0.08	
<b>The Baltic Sea</b>				<b>The Barents Sea</b>					
0-25	0.18	0.19	0.07	0.10	0.22	0.15	0.14	0.12	
25-50	0.42	0.48	0.18	0.23	0.45	0.57	0.33	0.39	
50-75	0.54	0.57	0.16	0.29	0.52	0.51	0.53	0.34	
>75	0.71	0.67	0.16	0.19	0.52	0.37	0.28	0.37	

The Monte-Carlo approach and use of expressions (6.3)-(6.5) make it possible to reproduce the whole variety of values of function  $\Xi$ :

$$\begin{aligned} \mathcal{S}_k &= F_{\mathcal{S}}^{-1}(\gamma_1^{(k)}), \quad \Theta_k = F_{\Theta}^{-1}(\gamma_2^{(k)}) \\ h_k^+ &= F_{h^+/\mathcal{S}}^{-1}(\gamma_3^{(k)} | \mathcal{S}_k), \quad h_k^- = F_{h^-/\Theta}^{-1}(\gamma_4^{(k)} | \Theta_k) \end{aligned} \quad (6.8)$$

Here  $\{\gamma_i^{(k)}\}$  denotes a system of four pseudo-random numbers.

Using a sample of  $\Xi$  as a set of impulse parameters in expression (1.7) one can get a stochastic model for a sequence of storms and weather windows. Fig. 6.4 compares correlation functions  $K^*(\tau)$  computed by empirical data and impulse model (1.7) with the parameters estimated by (6.8). The similarity between correlation functions of the simulated process and empirical data depends, in a general case, on the shape of the impulse, the correlation between parameters

$\Xi = (h^+, h^-, \mathcal{S}, \Theta)t$ , and on the probability distributions  $\Xi t, \Xi s$  for various thresholds.

The correlograms in fig. 6.4 are computed using the impulse process model (1.7) accounting for the correlation (6.8) between parameters  $\Xi$  but not the correlation between  $\Xi t$  and  $\Xi s$  of the sequence of impulses. The figures show good agreement between variances of the simulated and observed process and times of the first zero level crossing.

Let us consider the dependence between two consecutive impulses using a storm classification based on instrumental wave observations in the Black Sea. The data came from a directional wave-rider installed at depth of about 85 m off the town of Gelendzhik. The measurements were recorded every three hours, and every hour during storms. The duration of each record is 20 minutes. The total duration of the series is approximately three years, and it contains more than 6000 wave height records ranging from 0 up to 8.5 m.

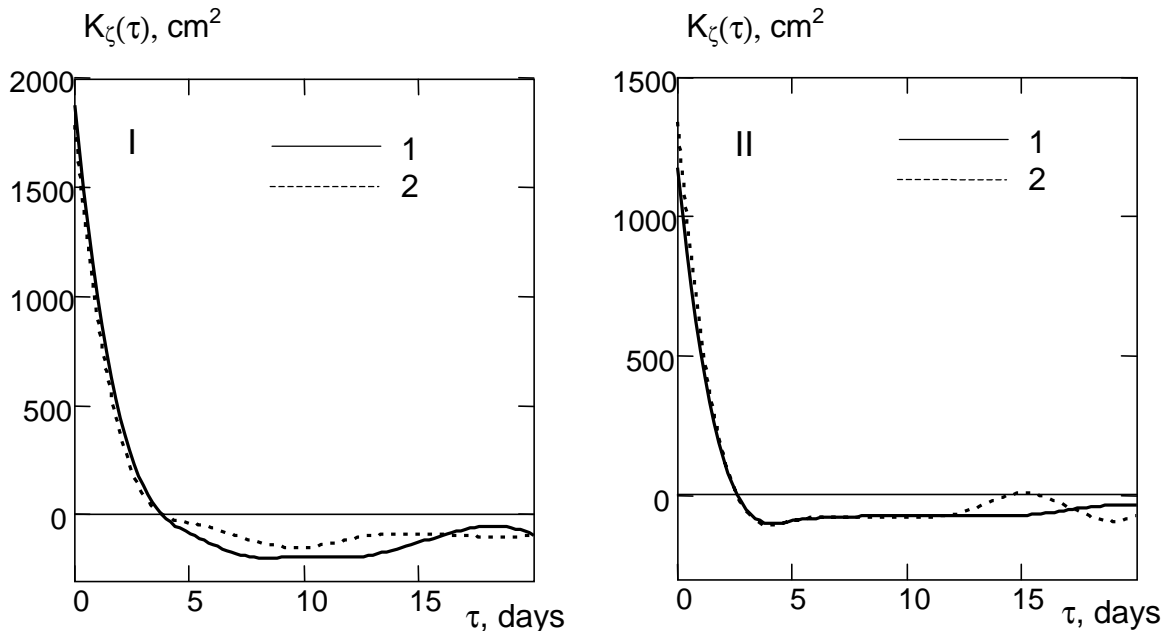


**Figure 6.4.** Estimates of wave height correlation function on synoptic time scales for Baltic (I) and Black (II) Seas. 1: impulse model, 2: empirical data

The data analysis shows that storm shapes are quite diverse and there are many ways to classify them. The classification results will depend significantly on the selection of  $Z$ . For smaller values of  $Z$ , shapes are increasingly variable, while for larger values of  $Z$  they become more uniform.

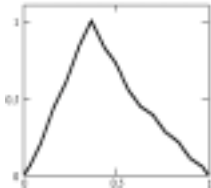
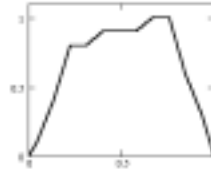
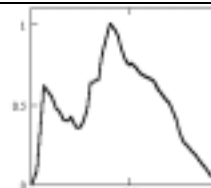
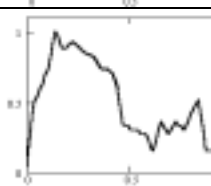
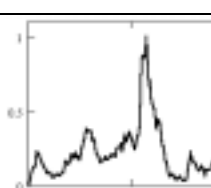
In [Boukhanovsky, Lavrenov, et al., 1999] five storm classes were specified (see Table 6.5). The dominating categories correspond to fully developed seas (I), and to wind waves not fully developed due to limitations of fetch or wind duration (II). The categories III and IV correspond to combined waves.

Storms of category V, which are defined as series of storms with wave heights exceeding a threshold  $Z$ , usually have the longest duration. Doubling of  $Z$  leads to almost complete disappearance of storm category V so that only four first categories remain.

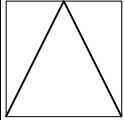
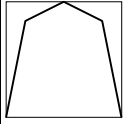
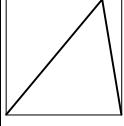
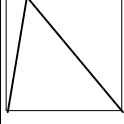
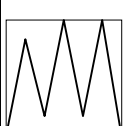
B.V. Divinsky used methods of discriminant analysis and came up with a more detailed classification of storms than is given in Table 6.5. He proposed eight types of storms for wave heights exceeding mean seasonal wave height  $h=Z$  and four types for wave heights exceeding  $h=2Z$  and  $h=3Z$ . These are given in Table 6.6. Further, B.V. Divinsky considered the correspondence between each storm type and dominating meteorological conditions. It is worth mentioning that, in spite of differences in the classification methods, the whole set of storm shapes for wave heights exceeding  $h=2Z$  fell almost similarly into four groups. Some differences in percentage in Tables 6.5 and 6.6 are due to varying criteria for attributing a storm to a certain category.

Weather windows can also be classified similarly. Table 6.7 shows a corresponding classification proposed by B.V. Divinsky.

**Table 6.5**  
*A classification of storm shapes*

Category	Non-dimensional shape abscissa is $(t-t_0)/S$ , ordinate is $h/h^+$	Threshold $Z=1.0 \bar{h}(t)$ where $\bar{h}(t)$ is seasonal mean wave height				Threshold $Z=2.0 \bar{h}(t)$ where $\bar{h}(t)$ is seasonal mean wave height			
		P, %	N	Wave height $h$ (cm)	Duration $S$ (hour)	P, %	N	Wave height $h$ (cm)	Duration $S$ (hour)
I		50%	110	$h_{95\%}=207$ $m_h=61$ $\sigma_h=57$ $h_{5\%}=21$	$S_{95\%}=45.5$ $m_S=11.0$ $\sigma_S=14.2$ $S_{5\%}=1.0$	49%	78	$h_{95\%}=241$ $m_h=105$ $\sigma_h=59$ $h_{5\%}=44$	$S_{95\%}=25.8$ $m_S=6.9$ $\sigma_S=8.0$ $S_{5\%}=0.7$
II		15%	33	$h_{95\%}=203$ $m_h=84$ $\sigma_h=54$ $h_{5\%}=22$	$S_{95\%}=71.7$ $m_S=28.7$ $\sigma_S=22.4$ $S_{5\%}=5.0$	24%	38	$h_{95\%}=267$ $m_h=121$ $\sigma_h=63$ $h_{5\%}=43$	$S_{95\%}=38.3$ $m_S=14.8$ $\sigma_S=10.3$ $S_{5\%}=1.8$
III		6%	13	$h_{95\%}=273$ $m_h=138$ $\sigma_h=75$ $h_{5\%}=33$	$S_{95\%}=95.5$ $m_S=44.9$ $\sigma_S=25.4$ $S_{5\%}=8.5$	13%	20	$h_{95\%}=207$ $m_h=137$ $\sigma_h=61$ $h_{5\%}=66$	$S_{95\%}=36.0$ $m_S=19.6$ $\sigma_S=11.0$ $S_{5\%}=5.0$
IV		19%	41	$h_{95\%}=273$ $m_h=108$ $h=63$ $h_{5\%}=44$	$S_{95\%}=82.5$ $m_S=40.9$ $s=23.3$ $S_{5\%}=12.2$	13%	20	$h_{95\%}=277$ $m_h=134$ $h=60$ $h_{5\%}=42$	$S_{95\%}=110.5$ $m_S=34.0$ $s=25.1$ $S_{5\%}=3.5$
V		10%	22	$h_{95\%}=197$ $m_h=104$ $h=64$ $h_{5\%}=31$	$S_{95\%}=135.8$ $m_S=70.0$ $s=41.5$ $S_{5\%}=9.5$	1%	2	$h_{95\%}=181$ $m_h=181$ $h=1$ $h_{5\%}=180$	$S_{95\%}=184.5$ $m_S=118.8$ $s=65.7$ $S_{5\%}=53.1$

**Table 6.6**  
A classification of storm shapes based on discriminant analysis

Type	Shape	Description	Threshold					
			1h	2h	3h	1h	2h	3h
			Number of storms			%		
I		Monotonic increase and decrease of wind	39	21	14	20.3	23.1	41.2
II		Stable wind at phase of maximal storm development	40	39	4	20.8	42.9	11.8
III		Duration of increase is considerably longer than one of decrease. This type is specific for "slow" storms	33	16	7	17.1	17.6	20.6
IV		Expressed asymmetry of the shape with domination of the decrease phase. This type is specific for "quick" storms	37	15	9	19.3	16.4	26.4
V		The discriminant analysis gives a separate type for this storm shape. It bears some similarity to type IV. This shape is typical for fast and deep cyclones	12	*	*	6.3	*	*
VI		Intermittent increase and decrease of waves caused by instabilities of the atmospheric flow. They are typical for a shallow or a slow moving cyclone	8	*	*	4.2	*	*
VII		Passage of a deep cyclone with distinct separation of fronts. Depending on the cyclone track wind wave field either develops having swell as its background or generates swell as a residual signal	19	*	*	9.9	*	*
VIII		A "chain" of storms, which cannot be separated due to small threshold value of Z	4	*	*	2.1	*	*

A matrix of probabilities that a certain storm category in Table 6.5 (for  $h=Z$ ) will transform into another category is shown in Table 6.8 It follows from the table that there is some weak correlation between categories of consecutive storms.

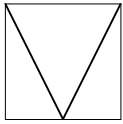
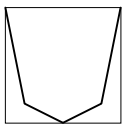
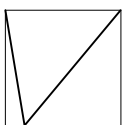
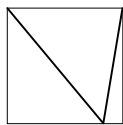
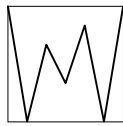
The annual cycle of storms manifests itself in variations of monthly mean wave height  $\bar{h}(t)$  between seasons. Also, synoptic variability is higher in winter than in summer.

Such cyclical variations can be expressed as

$$\xi(t) = m(t) + \sigma(t)[\xi_t + \eta(t)] \quad (6.9)$$

where  $m(t)$  is the multi-year norm (i.e. annually averaged value) of mean wave height. It is equal to the mathematical expectation of the periodically correlated random process.  $\sigma(t)$  is r.m.s. deviation of monthly mean wave heights from  $m(t)$ . The process  $\xi(t)$  can be modelled by (I.8)-(I.9) or (I.10)-(I.11). Lastly,  $\eta(t)$  is an impulse-like random process, which can be represented by (I.7) with parameters (6.8).

**Table 6.7**  
A classification of weather windows

Type	Shape	Description	Threshold					
			1h	2h	3h	1h	2h	3h
			Number of weather windows			%		
I		Smooth decrease and then increase of storm activity	31	22	16	14.9	22.2	47.1
II		Wind waves in the "window" are much weaker than the selected threshold value $h$	67	17	14	32.2	17.2	41.2
III		Gradual increase of storm activity or result of passage of a chain of storms with different tracks	39	14	*	18.8	14.1	*
IV		Strong residual wave field that is decaying after storm passage	49	16	*	23.6	16.2	*
V		Wave heights close to the threshold value $h$	22	30	4	10.5	30.3	11.7

**Table 6.8.**  
Probability matrix of transformation of one storm category into another

Storm category	I	II	III	IV	V
I	0.5	0.1	0.1	0.2	0.1
II	0.3	0.1	0.2	0.2	0.2
III	0.6	0.2	0.1	0.1	---
IV	0.3	0.2	0.2	0.3	---
V	0.2	0.3	0.2	0.4	---

---oooOooo---